

# Theoretical and experimental analyses of Young's modulus and thermal expansion coefficient of the alumina-mullite system

Yoshihiro Hirata\*, Shota Itoh, Taro Shimonosono, Soichiro Sameshima

Department of Chemistry, Biotechnology, and Chemical Engineering, Kagoshima University, 1-21-40 Korimoto, Kagoshima, 890-0065 Japan

## ARTICLE INFO

### Article history:

Received 25 May 2016

Received in revised form

29 July 2016

Accepted 29 July 2016

### Keywords:

C. Mechanical properties

C. Thermal expansion

D.  $\text{Al}_2\text{O}_3$

D. Mullite

## ABSTRACT

Young's moduli ( $E$ ) and thermal expansion coefficients (TECs) of the alumina–mullite–pore system (96.4–99.5% relative density) were measured for a wide mullite fraction range from 0 to 100 vol%. Both  $E$  and TEC values decreased at high mullite fractions. These properties were theoretically analyzed with four proposed model structures that were constructed by three-phase systems of mullite (or alumina) continuous phase 2–pore dispersed phase 1–alumina (or mullite) dispersed phase 3. The ratios of  $E(\text{theoretical})/E(\text{experimental})$  and  $\text{TEC}(\text{theoretical})/\text{TEC}(\text{experimental})$  were very close to unity, depending on the mullite fraction. That is, the measured  $E$  and TEC values are closely related to the change in the composite microstructure as a function of mullite fraction.

© 2016 Elsevier Ltd and Techna Group S.r.l. All rights reserved.

## 1. Introduction

In a previous study [1], we proposed theoretical effective linear thermal expansion coefficients (TECs) of solid material with simple cubic particulate inclusion (size  $a$ ) for two model structures: a parallel structure (Fig. 1(b)) and a series structure (Fig. 1(c)) of laminated layers. The number ( $p$ ) of inclusions along one direction of cubic composite in Fig. 1(a) is equal to  $V^{1/3}/a$ , where  $V$  is the volume fraction of inclusions, and the distance between two inclusions is given by  $(1/p - a)$ . The detailed derivation of the Young's modulus ( $E_c$ ) and TEC ( $\beta_c$ ) for the model structure of Fig. 1(b) or Fig. 1(c) is reported in our previous study [1]. Tables 1 and 2 represent the finally derived mixing rules of  $E$  and  $\beta$  values for dispersed cubic phase 1 and continuous phase 2. In the parallel model structure (Fig. 1(b)), the distinguishment of dispersed and continuous phases is not required; only the fraction of included phase is important to the calculation of  $\beta_c$  in Table 1. The  $\beta_c$  curve as a function of volume fraction of dispersed phase changes with a small curvature. In the series structure (Fig. 1(c)), the distinguishment of the dispersed and continuous phases provided different calculated  $\beta_c$  curves with a large curvature. In our previous paper [1], a very good agreement was observed between the experimental and theoretical (series model) TECs of the W–MgO system. Compared to the previously developed Turner's equation and Kerner's equation, the mixing rule in Table 2 is closer to the experimental TEC of the W–MgO system.

TEC of a composite is closely related to its Young's modulus, as is evident in Tables 1 and 2. However, fabricating a dense ceramic composite with no porosity is difficult; thus, composites composed of three-phase systems (continuous solid phase–dispersed solid inclusion–dispersed pores) tend to be obtained. Fortunately, the TEC equation in Table 1 or Table 2 is easily extended to a multi-phase system [1–3]. In the three-phase system of a dispersed phase 1 (with volume fraction  $V_1$ ), continuous phase 2 (with volume fraction  $V_2$ ), and dispersed phase 3 (with volume fraction  $V_3$ ), we first calculate  $E_c$  and  $\beta_c$  for the two-phase system of a dispersed phase 1 and a continuous phase 2 using the given volume fractions of  $V_1$  and  $V_2$  in the three-phase system ( $V_1 + V_2 + V_3 = 1$ ). That is, the  $V$  of dispersed phase 1 in Table 1 or Table 2 is changed to the ratio  $V_1/(V_1 + V_2)$ . Here, we treat this composite that includes phases 1 and 2 as a new continuous phase and again treat the calculated  $E_c$  and  $\beta_c$  as  $E_2(\text{new})$  and  $\beta_2(\text{new})$ , respectively. Phase 3 is dispersed in the new continuous phase with  $E_2(\text{new})$  and  $\beta_2(\text{new})$ . Therefore,  $E_1$ ,  $\beta_1$ ,  $V$ ,  $E_2$ , and  $\beta_2$  in Table 1 or Table 2 are changed to  $E_3$ ,  $\beta_3$ ,  $V_3$ ,  $E_2(\text{new})$ , and  $\beta_2(\text{new})$ , respectively, in the three-phase system. As previously mentioned, twice repeating the calculation summarized in Table 1 or Table 2 provides the Young's modulus and the TEC for the three-phase system. When a composite contains dispersed pores, the Young's modulus and TEC of pores are assumed to be 0 GPa and  $0 \text{ K}^{-1}$ , respectively [4].

In this paper, an important refractory composite of the alumina–mullite ( $3\text{Al}_2\text{O}_3 \cdot 2\text{SiO}_2$ ) system was fabricated by hot-pressing over a wide range of mullite volume fractions. According to the phase diagram of the  $\text{Al}_2\text{O}_3$ – $\text{SiO}_2$  system [5], mullite has a narrow solid solution range of 70.5–74.0 mass%  $\text{Al}_2\text{O}_3$ , and no compound is formed between alumina and mullite solid solution below 2101 K.

\* Corresponding author.

E-mail address: [hirata@cen.kagoshima-u.ac.jp](mailto:hirata@cen.kagoshima-u.ac.jp) (Y. Hirata).

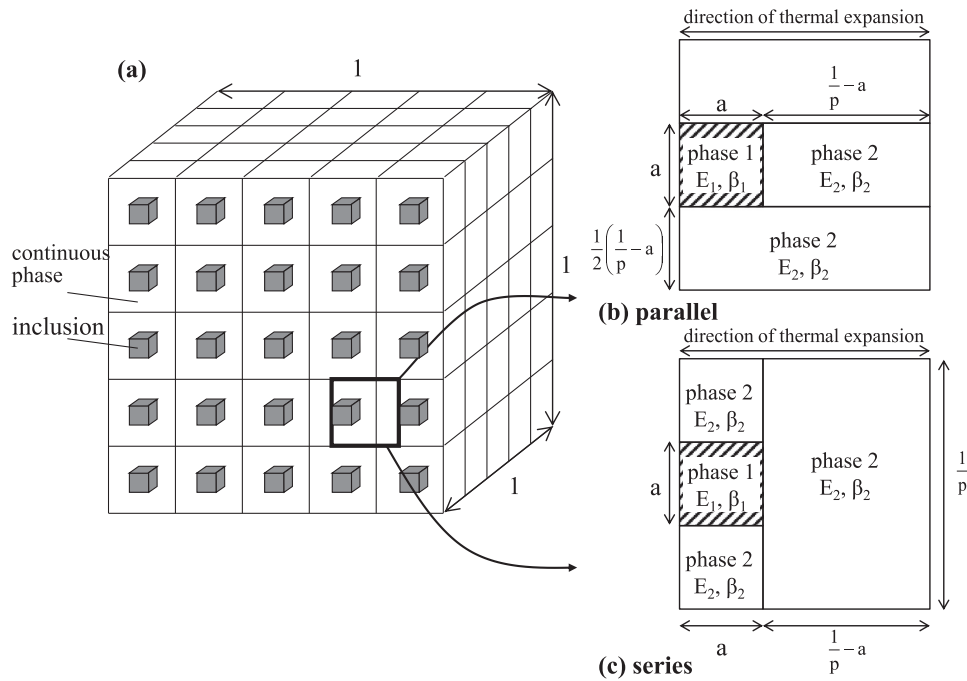


**Fig. 1.** (a) Model structure of material with a simple cubic inclusion. The geometrical features are shown in (b) parallel and (c) series structure models.  $E$  and  $\beta$  indicate the Young's modulus and thermal expansion coefficient of dispersed phase 1 or continuous phase 2, respectively.

**Table 1**

Summary of Young's modulus ( $E_c$ ) and thermal expansion coefficient ( $\beta_c$ ) of composite in a parallel structure shown in Fig. 1(b) [1].

$\beta_c = \frac{E_b V^{2/3} \beta_b + E_2 (1 - V^{2/3}) \beta_2}{E_b V^{2/3} + E_2 (1 - V^{2/3})}$	(1)
$E_c (\text{Denominator of equation}) = E_2 - E_2 V^{2/3} \left[ 1 - \frac{1}{1 - V^{1/3} \left( 1 - \frac{E_2}{E_1} \right)} \right]$	(2)
$E_b \text{ and } \beta_b \text{ in Eq. (1) are given by Eqs. (3) and (4), respectively}$	
$E_b = \frac{E_1 E_2}{E_2 V^{1/3} + E_1 (1 - V^{1/3})}$	(3)
$\beta_b = \beta_1 V^{1/3} + \beta_2 (1 - V^{1/3})$	(4)
$E_1: \text{Young's modulus of dispersed phase 1}$	
$E_2: \text{Young's modulus of continuous phase 2}$	
$E_c: \text{Young's modulus of composite (b) in Fig. 1(b)}$	
$V: \text{Volume fraction of dispersed phase 1}$	
$\beta_1: \text{Thermal expansion coefficient of dispersed phase 1}$	
$\beta_2: \text{Thermal expansion coefficient of continuous phase 2}$	
$\beta_c: \text{Thermal expansion coefficient of composite (b) in Fig. 1(b)}$	

**Table 2**

Summary of Young's modulus ( $E_c$ ) and thermal expansion coefficient ( $\beta_c$ ) of composite in a series structure shown in Fig. 1(c) [1].

$\beta_c = \left( \frac{E_d}{E_c} \right) \beta_d$	(5)
$\frac{1}{E_c} = \frac{V^{1/3}}{E_d} + \frac{1 - V^{1/3}}{E_2}$	(6)
$E_d \text{ and } \beta_d \text{ in Eq. (5) are given by Eqs. (7) and (8), respectively}$	
$E_d = E_1 V^{2/3} + E_2 (1 - V^{2/3})$	(7)
$\beta_d = \frac{E_1 V^{2/3} \beta_1 + E_2 (1 - V^{2/3}) \beta_2}{E_1 V^{2/3} + E_2 (1 - V^{2/3})}$	(8)
$E_1: \text{Young's modulus of dispersed phase 1}$	
$E_2: \text{Young's modulus of continuous phase 2}$	
$E_c: \text{Young's modulus of composite (c) in Fig. 1(c)}$	
$V: \text{Volume fraction of dispersed phase 1}$	
$\beta_1: \text{Thermal expansion coefficient of dispersed phase 1}$	
$\beta_2: \text{Thermal expansion coefficient of continuous phase 2}$	
$\beta_c: \text{Thermal expansion coefficient of composite (c) in Fig. 1(c)}$	

This system is suitable for comparing the measured and calculated TECs. Because the mullite powder used in these experiments contained 71.46 mass%  $\text{Al}_2\text{O}_3$ , a small amount of the mixed alumina might dissolve into mullite grains during sintering. However, the influence of the dissolved alumina on the Young's modulus

and TEC of the alumina–mullite system is not discussed in this paper due to the difficulty in experimentally detecting the small change in the Young's modulus and TEC upon the formation of mullite solid solution. In these experiments, the composite was densified to 96.4–99.5% relative density by hot-pressing at 1773–1923 K. The Young's moduli and TECs of the composite parallel and perpendicular to the direction of hot-pressing were measured at

Download English Version:

<https://daneshyari.com/en/article/5438766>

Download Persian Version:

<https://daneshyari.com/article/5438766>

[Daneshyari.com](https://daneshyari.com)